

Iron Oxide Nanoparticles in a Dynamic Flux: Magnetic Hyperthermia Effect on Flowing Heavy Crude Oil

Maria E. F. Brollo,* Ivanei F. Pinheiro, Gabriel S. Bassani, Guillaume Varet, Daniel Merino-Garcia, Vanessa C. B. Guersoni, Marcelo Knobel, Antonio C. Bannwart, Charlie van der Geest, and Diego Muraca*



Cite This: *ACS Omega* 2023, 8, 32520–32525



Read Online

ACCESS |



Metrics & More

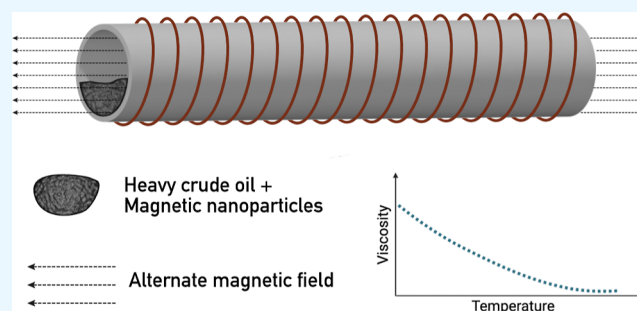


Article Recommendations



Supporting Information

ABSTRACT: An essential part for crude oil extraction is flow assurance, being critical to maintain a financially sustainable flow while getting the petroleum to the surface. When not well managed, it can develop into a significant issue for the O&G industry. By heating the fluids, problems with flow assurance, including paraffin deposition, asphaltene, and methane hydrate, can be reduced. Also, as the temperature rises, a liquid's viscosity decreases. Research focusing on the application of magnetic nanoparticles (NPs) in the oil industry is very recent. When magnetic nanofluids are exposed to an alternating magnetic field, the viscosity decreases by several orders of magnitude as a result of the fluid's temperature rising due to a phenomenon known as magnetic hyperthermia. This work focuses on the use of magnetic NPs (9 nm) in heavy crude oil (API 19.0). The frequency and strength of the magnetic field, as well as the characteristics of the fluid and the NPs intrinsic properties all affect the heating efficiency. For all of the experimental settings in this work, the flowloop's temperature increased, reaching a maximum of $\Delta T = 16.3$ °C, using 1% wt NPs at the maximum available frequency of the equipment (533 kHz) and the highest field intensity for this frequency (14 kA/m), with a flow rate of 1.2 g/s. This increase in temperature causes a decrease of nearly 45% on the heavy crude oil viscosity, and if properly implemented, could substantially increase oil flow in the field during production.



INTRODUCTION

Research on the use of magnetic nanoparticles (NPs) in the oil industry is relatively uncommon yet. However, this approach presents possible solutions to problems of flow assurance,^{1–5} separation between water and oil,^{6–9} asphaltenes adsorption,^{10–12} and growth of wax crystals.^{13,14}

During the extraction and transport of crude oil from the offshore wells, the pipes (filled with the crude oil and natural gas) pass through the seabed at 4 °C, precipitating solid materials and depositing them on the inner walls of those pipes in a combination of complex processes.¹⁵ Such solid deposits can include wax, hydrates, and asphaltenes,¹⁶ where flow can be severely restricted or even completely stopped, leading to various environmental, safety, health, and economic risks. As an estimated expense example, a well cleaning operation in the Gulf of Mexico costed approximately US\$ 70 million/well.¹⁷ Remedying these problems currently makes use of chemical inhibition methods,¹⁵ which prevent the precipitation and deposition of these solids. These methods require the continuous injection of inhibitors, which could not only be dangerous but also add problems to the process downstream. Other frequent technique includes “pigging,”^{18,19} which directly hinders production because the flow must be stopped

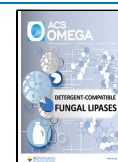
during the procedure and the tool is prone to getting stuck in the pipes.

This research focuses on a different approach to the flow assurance problems in oil production, by adding magnetic nanoparticles to the oil flowing in the pipes, and with the subsequent application of an alternating magnetic field (AMF) to the system.²⁰ Here, the nanoparticle (NP) concentration of the heavy crude oil was changed. A phenomenon known as magnetic hyperthermia occurs when a magnetic monodomain nanoparticle (or ferro(i)magnetic) is subjected to an AMF that, depending on its strength and frequency (higher than relaxation time), will generate irreversibility in the magnetization loop, releasing energy into the medium in the form of heat.^{21–24} Heat comes from two different mechanisms when the NPs are in a colloidal suspension: the so-called Néel and Brownian relaxations. Néel relaxation is related to coherent

Received: April 25, 2023

Accepted: July 13, 2023

Published: August 28, 2023



rotation of the nanoparticle magnetic moments and will depend on effective anisotropy and temperature,^{25,26} while the heat generated by the physical rotation of particles due to the process of aligning magnetic moments with the external AMF refers to the Brownian mechanism.^{27,28} Heat efficiency can be improved by specifically adjusting intrinsic NP properties, the colloidal properties, or even the AMF conditions as intensity and frequency. It is well known that by increasing a fluid's temperature, its viscosity decreases.^{29,30} So, the application of AMF on fluids with added NPs can tune their viscosity, eventually leading to a decrease of several orders of magnitude.³¹

The specific experimental setup was designed to be orders of magnitude bigger than the usual setups used in magnetic hyperthermia.^{32–34} It is worth noting that our experiment adds another complex variable: the nanoparticles dispersed in the oil are flowing through a pipe, subjected to an AMF.

The main contribution of this work is to demonstrate that it is possible to change the properties of crude oil through magnetic hyperthermia, namely reducing its viscosity and increasing its flow rate, which would lead to a reduction in formation of paraffin crystals, for example. This is a continuation of a previous work where the same magnetic nanoparticles were tested in diesel as a first proof of concept,²⁰ using the same flowloop configuration. Diesel at room temperature has a viscosity of 4.7 mPa·s, while the heavy crude oil used here has a viscosity of 124.3 mPa·s at room temperature. This work adds a layer of complexity to the system, since this viscous liquid contains saturates, aromatics, resins, and asphaltenes. Thinking on the real application, it would be possible to recover nanoparticles at the end of the process, employing a static magnetic field. This would allow their partial reuse, reducing the operational costs and contributing to make this technology viable. It is worth mentioning that the same idea can, in principle, be applied to any industry that depends on a flux of a viscous fluid.

MATERIALS AND METHODS

The tools and techniques utilized to identify and investigate the hyperthermia in magnetic colloids are all explained in this section. Repsol Sinopec Brazil provided the heavy crude oil (API gravity of 19.0) and NanoGap provided the 9 nm iron oxide (Fe₃O₄) NP for this study. Oleic acid-coated and oleic acid-dispersed nanoparticles were delivered with a weight concentration of 12%. Saturation magnetization (MS) values are 71 A m²/kg NP at 300 K, measured in a previous work.²⁰ Toluene (C₆H₅CH₃, ≥99.5%) and oleic acid (C₁₈H₃₄O₂, ≥90%) were both acquired from Sigma-Aldrich and used without further processing. The diesel (type S10) was purchased from commercial vendors and filtered to remove contaminants. There was no further special process carried out.

Fluid Characterization. The first procedure was to characterize the crude oil with a SARA standard measurement, described in Table S1. Heavy crude oil present 11.9% of saturated content. Diesel and heavy crude oil measured from 10–25 °C had the Arrhenius law (exponential increase as the temperature decrease) validated.

Differential Scanning Calorimetry. The specific heat (c_p) of heavy oil was measured using a differential scanning calorimetry (DSC) (Q2000, TA Instruments, USA), and the experiments were based on ASTM E1269–05. The sample was scanned from 0 to 140 °C with nitrogen atmosphere and 20 °C/min of heating rate. Three stages of measurement were

used; baseline, reference (sapphire), and sample. The c_p of was calculated using the library software (TA instruments).

Rheological Properties. The fluids' viscosity was measured using a controlled stress rheometer (Thermo, Haake Mars), employing a cone and plate geometry with a diameter of 60 mm and a cone angle of 1° with a gap of 0.052 mm. Shear stress and dynamic viscosity were measured at different shear rates roughly ranging from 5 to 200 s⁻¹.

Colloidal Preparation. Here, 9 nm oleic-coated iron oxide nanoparticles were supplied by NanoGap. The NPs were sonicated for 5 min in ultrasonic bath as received from supplier. Then, NPs were dispersed into diesel by sonicating another 5 min. The final nanocolloids were prepared in heavy crude oil, using a turrax mixer for 2 min at 10 000 rpm and then sonicating for an additional 5 min, in three different concentrations (0.5, 0.75, and 1% wt, respectively) in order to assess the effect of concentration on heating performance.

Transmission Electron Microscopy. Transmission electron microscopy (TEM) was performed in a JEM 2100 transmission electron microscope, with 200 kV accelerating voltage. On a copper grid with carbon coating, a drop of the suspension (nanoparticles in toluene) was placed, enabling the solvent to evaporate at room temperature. Across a population of more than 300 nanoparticles, the size distribution was determined from various photographs using the ImageJ software.

Magnetic Hyperthermia. To measure the magnetic hyperthermia of the colloids, NanoScale Biomagnetics G3 Series equipment was used to generate an alternate magnetic field. To eliminate magnetic field interference, an optical fiber sensor (OSENSA's FTX) was employed as the temperature probe. The coil used had a length of 343 mm and a diameter of 32 mm. The experimental setup was a closed flowloop designed as a prototype, explained in more detail in Brollo et al.²⁰ with a picture described in Figure S1. Its components include a tank (with a maximum 8 L capacity and a temperature range of ambient to 60 °C), a booster pump, the test area, and a heat exchange system. For the tests, a magnetic colloid was introduced to the tank, the pump is followed by the Coriolis flowmeter, where the mass flow rate (with an upper and lower limit of 3.6 and 1.2 g/s, respectively) and density of the mixture are measured. Before entering the test section, pressure and temperature are constantly being checked. The primary measurement is the temperature difference between the input and output. As a metallic sensor, the PT100 was mounted 0.5 m away from the coil to minimize any potential magnetic field effects. The error in temperature control is ±1 °C. Before each test, the mixture is allowed to flow for 1 h, stabilizing the temperature. Following this homogenization, the NanoScale Biomagnetics driver G3 was activated at the specified frequencies and field intensity. Data was gathered for 20 min. In order to homogenize and stabilize the temperature for the following experimental point, the driver G3 was turned off after the experiment.

RESULTS AND DISCUSSION

The main idea of this work is to examine the effect of concentration when a heavy crude oil with dispersed NPs flows under an AMF, using different magnetic field frequencies, magnetic field intensities, and fluid flow rates. TEM images of these nanoparticles can be found in Figure S2, on Supporting Information.

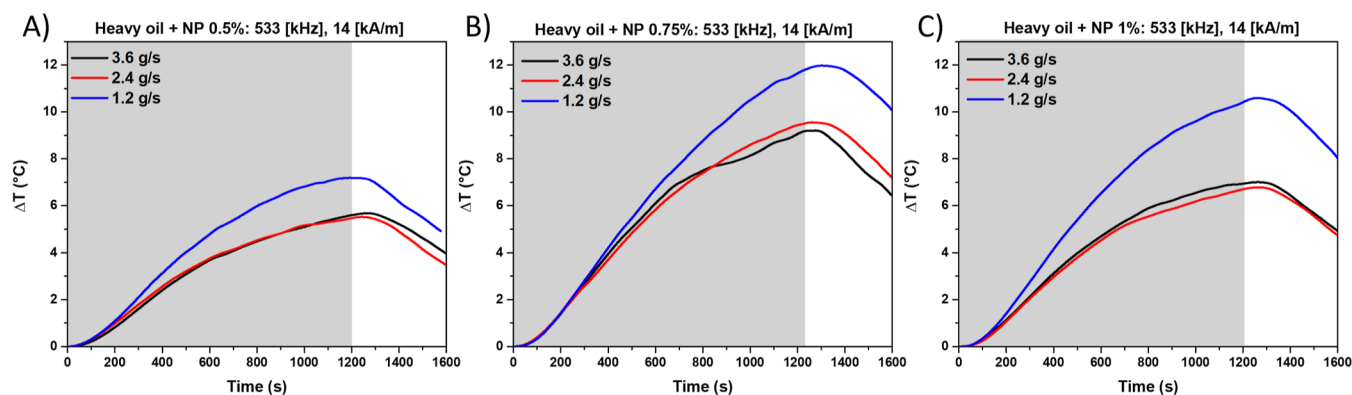


Figure 1. Temperature variation as a function of time, for different liquid flow rates, keeping constant the field intensity (14 kA/m) and frequency (533 kHz). (A) Heavy oil with 0.5% wt of NPs, (B) heavy oil with 0.75% wt of NPs, and (C) heavy oil with 1% wt of NPs. Blue curves represent the slowest flow rate available (1.2 g/s) while black curve represents the faster flow rate available (3.6 g/s). Gray area represents the application time of the AMF (1200 s).

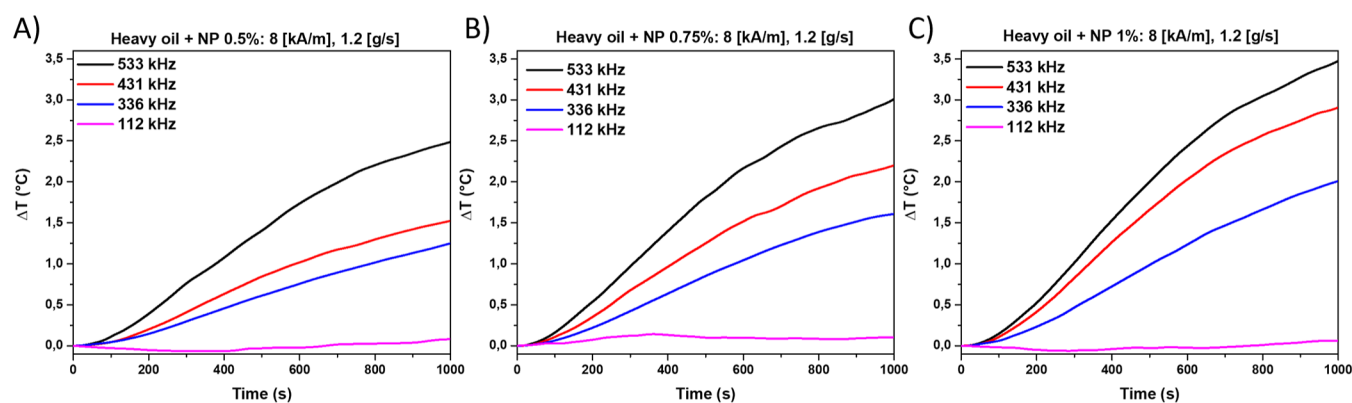


Figure 2. Temperature increase as a function of time, for different field frequencies, keeping constant the field intensity (8 kA/m) and flow rate (1.2 g/s). (A) Heavy oil with 0.5% wt of NPs, (B) heavy oil with 0.75% wt of NPs, and (C) heavy oil with 1% wt of NPs. The black curve represents the higher frequency available (533 kHz) while the pink curve represents the lower frequency available (112 kHz).

In Figure 1, the increase in temperature is shown as a function of the active magnetic field time (gray area), with constant field intensity of 14 kA/m and constant frequency of 533 kHz. It is also possible to verify the influence of the residence time and the NP concentration on temperature increase. Figure 1A shows 0.5% wt NPs, Figure 1B shows 0.75% wt NPs, and Figure 1C shows 1% wt NPs, respectively. The results show that an increase in NP concentration provides an increase in temperature, reaching a maximum ΔT of 12 °C. Also, as the mass flow rate drops, the NPs are exposed to the magnetic field for longer periods of time, which raises the fluid's temperature. The fact that the particles are not isolated facilitates them to aggregate into bigger clusters, where the magnetic dipole interaction between them can influence the behavior of the individual particles. This might be the source on the temperature difference seen between 0.75 and 1% wt NP. This was discussed in more detail in a previous work.³¹

Figure 2 shows the direct increase in temperature with rising magnetic field frequency, keeping the field intensity constant at 8 kA/m and the flowrate at 1.2 g/s. Figure 1A shows 0.5% wt NPs, Figure 1B shows 0.75% wt NPs, and Figure 1C shows 1% wt NPs, respectively. For the lowest frequency available at the NanoScale equipment (112 kHz, pink curve), the temperature increase is independent of NP concentration. A clear difference in temperature increase is evidenced when the frequency to

which the nanoparticles are subjected is increased. The highest frequency available on the equipment is 533 kHz (black curves), reaching a point where the temperature difference is broader, achieving a maximum of 3.5 °C in 1000 s for the sample with 1% wt NPs.

In previous works, an important parameter in magnetic hyperthermia, the so-called specific absorption rate (SAR) of these systems (for static measurements) was discussed.^{20,31} The system's temperature variation was measured, and the energy output is given in W/g units. The system's heat dissipation was determined by the lower relaxation time between the Néel and Brownian mechanisms. The viscosity of the liquid and the NP hydrodynamic volume affect the Brownian contribution. On the other hand, the volume and NP anisotropy affect the Néel contribution. For the nanoparticles used in this work, the Néel relaxation time was calculated as τ_N ($\sim 1.9 \times 10^{-9}$ s). The size, shape, colloidal stability, and concentration of NPs all affect the final SAR values. Equations can be found in Supporting Information. The maximum ΔT value for heavy oil was 57 °C in 2 min, for 0.5% wt of NPs, under 28 kA/m and 770 kHz, respectively. This increase in temperature means a SAR value of 187 W/g. In this work, we were not calculating the SAR values because it is a dynamic system where this important parameter was not fully defined yet.

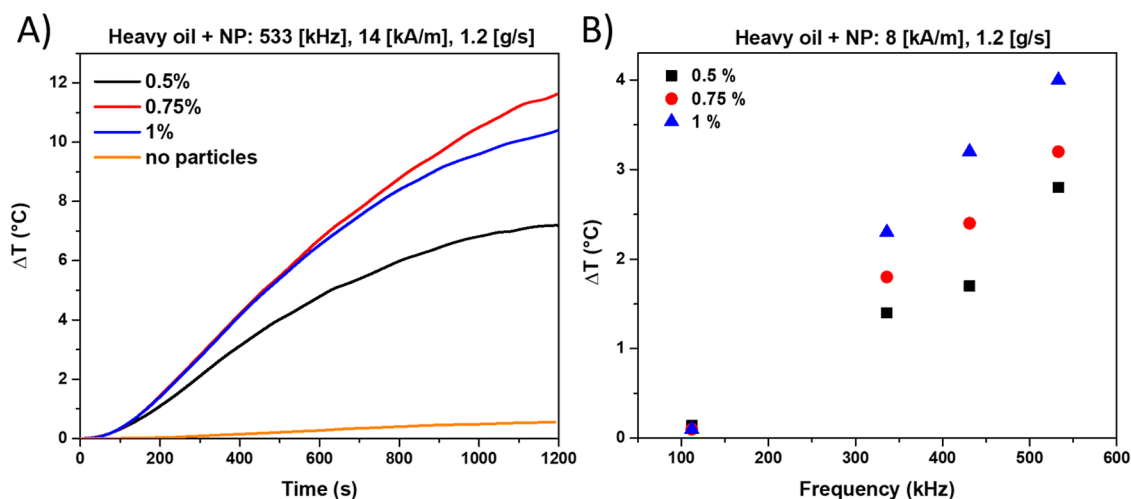


Figure 3. (A) Temperature increase as a function of time for different NP concentrations in heavy oil. Constant values for field intensity (14 kA/m), field frequency (533 kHz), and flow rate (1.2 g/s), respectively. (B) Temperature increase as a function of field frequency for different NP concentrations in heavy oil. Constant values for field intensity (8 kA/m) and flow rate (1.2 g/s). Applied magnetic field for 1200 s.

To evidence the effect of NPs concentration on the temperature increase, Figure 3A shows the temperature change ΔT as a function of time, maintaining constant the other variables: frequency at 533 kHz, field intensity at 14 kA/m, and flowrate at 1.2 g/s, respectively.

Indeed, Figure 3A shows that there is a negligible temperature increase in the measurement without adding nanoparticles to the oil (orange curve), indicating that an eventual temperature increase due to eddy current effect is not relevant. The heat observed on the magnetic colloids when the magnetic field is on, is indeed due to magnetic relaxation effects from the nanoparticles contained in the crude oil. Also, the increase in temperature is probably not due to the naturally occurring magnetic nanoparticles in the crude oil,¹⁴ since the same behavior was observed for a sample containing only diesel, presented in a previous work.²⁰ Figure 3B evidences the ΔT variation as a function of frequency, where the higher the frequency, the broader the temperature difference. Constant values of field intensity 8 kA/m and flow rate 1.2 g/s were maintained to keep apart the variable of interest. One observes a maximum difference in ΔT of more than 1 °C at the higher frequency by doubling the NP concentration, for the same magnetic field conditions.

Owing to a safety reason, there is an upper limit on the magnetic field application time (20 min). As a final experiment, a longer application time was tested to evaluate if an asymptotic behavior would be reached. Figure 4 shows this measurement, using the highest frequency available at the equipment (533 kHz), with the highest available field intensity for this frequency (14 kA/m), under the lowest flow rate (1.2 g/s), using 1% wt NPs and 50 min of magnetic field application time. The result was a remarkable increase in temperature of 16.3 °C, which is considerably higher than the results for 20 min.

In a previous work,³¹ we have measured viscosity vs temperature at constant shear rate for heavy crude oil. Previous data show the decrease in viscosity as the temperature increases, with Newtonian behavior, following an exponential increase with the decrease in temperature. These findings provide a simple way to connect how the heat emitted by NPs can alter the fluid's viscosity by showing a direct correlation between temperature and viscosity. Using data from the

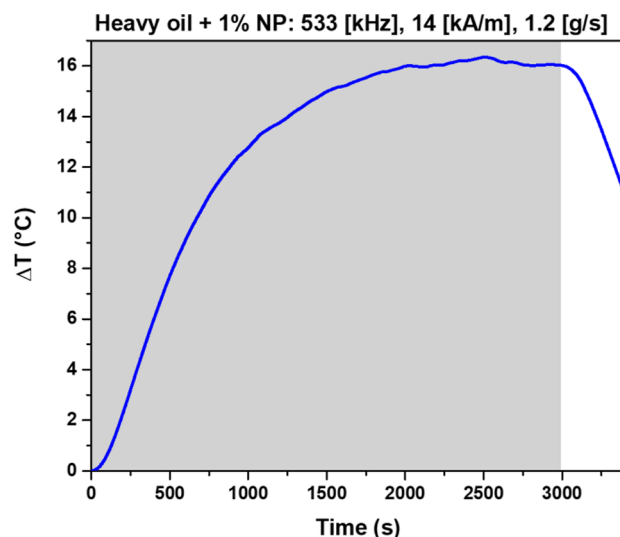


Figure 4. Temperature increase as a function of time for heavy oil with 1% wt of NPs, keeping constant the field intensity (14 kA/m), frequency (533 kHz), and flow rate (1.2 g/s), respectively. Gray area indicates the application time for the AMF (3000 s).

literature,³¹ it is possible to predict that a temperature increase of 16.3 °C would lead to a reduction of nearly 45% on the heavy oil viscosity.

CONCLUSIONS

This work presents the findings of an experimental investigation into the hyperthermia effect when commercial heavy crude oil flowing under an AMF is mixed with superparamagnetic nanoparticles. The goal of the study was to determine how NP concentration affected crude oil by calculating the amount of heat that was transferred to the fluid. The application of heat can be controlled remotely, thanks to this technology. The impact of the NP concentration is evident. If the system is colloidally stable, the hyperthermia response grows as the concentration does. When concentration and flow rate were held constant, the temperature variation (ΔT) in the flowloop rose linearly with frequency. For all of the experimental conditions for the heavy oil with added

nanoparticles, there was a temperature rise in the flowloop. The maximum temperature increase of 16.3 °C, observed between the inlet and outlet of the experimental section, was achieved using the highest frequency of the magnetic field available (533 kHz) and the highest field intensity for this frequency (14 kA/m). This temperature increase was achieved for a 50 min application period. The results presented here demonstrate the possibility of altering the properties of heavy crude oil through magnetic hyperthermia. By improving the recovery of nanoparticles along the production line, which can be reused, leading to significant savings of money and resources. Technology is in its infancy for this field, and it shows signs of a prosperous future not limited only to the O&G industry.

■ ASSOCIATED CONTENT

SI Supporting Information

The Supporting Information is available free of charge at <https://pubs.acs.org/doi/10.1021/acsomega.3c02832>.

SARA analysis of the heavy oil, full database for the experimental matrix on the dynamic results for temperature increase, TEM images of the iron oxide nanoparticles, picture with schematics on the experimental apparatus, and linear response theory explanation (PDF)

■ AUTHOR INFORMATION

Corresponding Authors

Maria E. F. Brollo – Physics Institute “Gleb Wataghin” (IFGW), University of Campinas (Unicamp), São Paulo 13083-859, Brazil; orcid.org/0009-0002-7191-1568; Email: brollo@ifi.unicamp.br

Diego Muraca – Physics Institute “Gleb Wataghin” (IFGW), University of Campinas (Unicamp), São Paulo 13083-859, Brazil; Email: dmuraca@unicamp.br

Authors

Ivanei F. Pinheiro – Center for Energy and Petroleum Studies (CEPETRO), University of Campinas (Unicamp), São Paulo 13083-896, Brazil

Gabriel S. Bassani – Repsol Sinopec Brazil, Rio de Janeiro, Rio de Janeiro 22250-040, Brazil

Guillaume Varet – Repsol, Madrid 28045, Spain

Daniel Merino-Garcia – Repsol, Madrid 28045, Spain

Vanessa C. B. Guersoni – Center for Energy and Petroleum Studies (CEPETRO), University of Campinas (Unicamp), São Paulo 13083-896, Brazil

Marcelo Knobel – Physics Institute “Gleb Wataghin” (IFGW), University of Campinas (Unicamp), São Paulo 13083-859, Brazil

Antonio C. Bannwart – School of Mechanical Engineering, University of Campinas (Unicamp), São Paulo 13083-860, Brazil

Charlie van der Geest – Center for Energy and Petroleum Studies (CEPETRO), University of Campinas (Unicamp), São Paulo 13083-896, Brazil; orcid.org/0000-0003-3469-2140

Complete contact information is available at:

<https://pubs.acs.org/doi/10.1021/acsomega.3c02832>

Notes

The authors declare no competing financial interest.

■ ACKNOWLEDGMENTS

We appreciate Repsol-Sinopec Brazil’s financial and technical assistance with this research. We appreciate the financial assistance provided by the ANP (National Agency of Petroleum, Natural Gas, and Biofuels) (21264-7). Also, we appreciate the assistance of the Laboratory of Materials and Low Temperature and the ALFA research team. The Laboratory for Analysis, Simulation, and Synthesis of Chemical Processes is acknowledged by the authors for its assistance with the study of DLS and AAS. The Brazilian Nanotechnology National Laboratory (LNNano) TEM facilities at Centro Nacional de Pesquisa em Energia e Materiais (CNPEM) and FAPESP (17/10581-1) and (2022/16460-0) are also acknowledged by the authors.

■ REFERENCES

- (1) Gharibshahi, R.; Omidkhan, M.; Jafari, A.; Mehrooz, N. Parametric optimization of in-situ heavy oil upgrading using simultaneous microwave radiation and magnetic nanohybrids via Taguchi approach. *Fuel* **2022**, *325*, 124717.
- (2) Davidson, A.; Huh, C.; Bryant, S. L. *Focused magnetic heating utilizing superparamagnetic nanoparticles for improved oil production applications*; OnePetro, 2012, SPE-157046-MS.
- (3) Ko, S.; Huh, C. Use of nanoparticles for oil production applications. *J. Pet. Sci. Eng.* **2019**, *172*, 97–114.
- (4) Mehta, P.; Huh, C.; Bryant, S. Evaluation of superparamagnetic nanoparticle-based heating for flow assurance in subsea flowlines. *International Petroleum Technology Conference, Kuala Lumpur, Malaysia*; OnePetro, 2014, IPTC-18090-MS.
- (5) Sabet, S. A.; Omidkhan, M.; Jafari, A. Viscosity reduction of extra-heavy crude oil using nanocatalysts. *Korean J. Chem. Eng.* **2022**, *39*, 1207–1214.
- (6) Zaman, H.; Shah, A. u. H. A.; Ali, N.; Zhou, C.; Khan, A.; Ali, F.; Tian, C. T.; Bilal, M. Magnetically recoverable poly (methyl methacrylate-acrylic acid)/iron oxide magnetic composites nanomaterials with hydrophilic wettability for efficient oil-water separation. *J. Environ. Manage.* **2022**, *319*, 115690.
- (7) Peng, J.; Liu, Q.; Xu, Z.; Masliyah, J. Novel Magnetic Demulsifier for Water Removal from Diluted Bitumen Emulsion. *Energy Fuels* **2012**, *26*, 2705–2710.
- (8) Ko, S.; Kim, E. S.; Park, S.; Daigle, H.; Milner, T. E.; Huh, C. Oil Droplet Removal from Produced Water Using Nanoparticles and Their Magnetic Separation. *SPE Annual Technical Conference and Exhibition, Dubai, UAE*; SPE, 2016, SPE-181893-MS.
- (9) Zhang, S.; Lü, T.; Qi, D.; Cao, Z.; Zhang, D.; Zhao, H. Synthesis of quaternized chitosan-coated magnetic nanoparticles for oil-water separation. *Mater. Lett.* **2017**, *191*, 128–131.
- (10) Daniela Contreras-Mateus, M.; Sanchez, F. H.; Cañas-Martínez, D. M.; Nassar, N. N.; Chaves-Guerrero, A. Effect of asphaltene adsorption on the magnetic and magnetorheological properties of heavy crude oils and Fe₃O₄ nanoparticles systems. *Fuel* **2022**, *318*, 123684.
- (11) Li, N.; Ke, H.; Wang, T.; Xia, S. Recyclable surface-functionalized Fe₃O₄ particles for heavy oil viscosity reduction. *J. Pet. Sci. Eng.* **2022**, *211*, 110112.
- (12) Mateus, L.; Taborda, E. A.; Moreno-Castilla, C.; López-Ramón, M. V.; Franco, C. A.; Cortés, F. B. Extra-Heavy Crude Oil Viscosity Reduction Using and Reusing Magnetic Copper Ferrite Nanospheres. *Processes* **2021**, *9*, 175.
- (13) Wang, N.; Daigle, H.; Prodanović, M. Simulating the Efficiency of Electromagnetic Pigging in Pipelines and Production Tubing Aided by Nanopaint. *SPE Annual Technical Conference and Exhibition, Calgary, Alberta, Canada*; SPE, 2022, SPE 196112.
- (14) Moscon, P. S.; Pessoa, M. S.; Rodrigues, M. C. R.; Alves, A. L.; Flores, E. M. M.; Passamani, E. C.; Vicente, M. A.; Santos, M. F. P. Investigation of the Naturally Occurring Magnetic Nanoparticles in

Crude Oil by AC Magnetic Susceptibility Experiment. *J. Supercond. Novel Magn.* **2021**, *34*, 2855–2863.

(15) Theyab, A. M. Fluid Flow Assurance Issues: Literature Review. *SciFed J. Pet.* **2018**, *2*, 1.

(16) Ellison, B. T.; Gallagher, C. T.; Frostman, L. M.; Lorimer, S. E. *The Physical Chemistry of Wax, Hydrates, and Asphaltene*; OnePetro, 2000, OTC-11963-MS.

(17) Farooq, U.; Patil, A.; Panjwani, B.; Simonsen, G. Review on Application of Nanotechnology for Asphaltene Adsorption, Crude Oil Demulsification, and Produced Water Treatment. *Energy Fuels* **2021**, *35*, 19191–19210.

(18) Schaefer, E. F. *Pigging of Subsea Pipelines*; Offshore Technology Conference, 1991.

(19) Li, W.; Huang, Q.; Wang, W.; Gao, X. Advances and Future Challenges of Wax Removal in Pipeline Pigging Operations on Crude Oil Transportation Systems. *Energy Technol.* **2020**, *8*, 1901412.

(20) Brollo, M. E. F.; Pinheiro, I. F.; Bassani, G. S.; Varet, G.; Guersoni, V. C. B.; Knobel, M.; Bannwart, A. C.; Muraca, D.; van der Geest, C. Iron Oxide Nanoparticles in a Dynamic Flux: Implications for Magnetic Hyperthermia-Controlled Fluid Viscosity. *ACS Appl. Nano Mater.* **2021**, *4*, 13633–13642.

(21) Dormann, J.-L.; Fiorani, D.; Tronc, E. *Advances in Chemical Physics*; Wiley, 1997; Vol. 98, pp 283–494. Magnetic Relaxation in Fine-Particle Systems

(22) Knobel, M.; Nunes, W.; Socolovsky, L.; De Biasi, E.; Vargas, J.; Denardin, J. Superparamagnetism and other magnetic features in granular materials: a review on ideal and real systems. *J. Nanosci. Nanotechnol.* **2008**, *8*, 2836–2857.

(23) Rosensweig, R. Heating magnetic fluid with alternating magnetic field. *J. Magn. Magn. Mater.* **2002**, *252*, 370–374.

(24) Shliomis, M. I. Magnetic fluids. *Sov. Phys.-Usp.* **1974**, *17*, 153–169.

(25) Néel, L. Théorie du trainage magnétique des ferromagnétiques en grains fins avec application aux terres cuites. *Ann. Geophys.* **1949**, *5*, 99–136.

(26) Néel, L. Théorie du trainage magnétique des substances massives dans le domaine de Rayleigh. *J. Phys. Radium* **1950**, *11*, 49–61.

(27) Brown, W. F. Thermal Fluctuations of a Single-Domain Particle. *Phys. Rev.* **1963**, *34*, 1319–1320.

(28) Brown, W. F. Thermal fluctuation of fine ferromagnetic particles. *IEEE Trans. Magn.* **1979**, *15*, 1196–1208.

(29) de Vicente, J.; Klingenberg, D. J.; Hidalgo-Alvarez, R. Magnetorheological fluids: a review. *Soft Matter* **2011**, *7*, 3701–3710.

(30) Aristizábal-Fontal, J. E.; Cortés, F. B.; Franco, C. A. Viscosity reduction of extra heavy crude oil by magnetite nanoparticle-based ferrofluids. *Adsorpt. Sci. Technol.* **2018**, *36*, 23–45.

(31) Pinheiro, I. F.; Brollo, M. E. F.; Bassani, G. S.; Varet, G.; Merino-García, D.; Guersoni, V. C. B.; Knobel, M.; Bannwart, A. C.; Muraca, D.; van der Geest, C. Effect of viscosity and colloidal stability on the magnetic hyperthermia of petroleum-based nanofluids. *Fuel* **2023**, *331*, 125810.

(32) Soto, P. A.; Vence, M.; Pinero, G. M.; Coral, D. F.; Usach, V.; Muraca, D.; Cueto, A.; Roig, A.; Van Raap, M. B. F.; Setton-Avruij, C. P. Sciatic nerve regeneration after traumatic injury using magnetic targeted adipose-derived mesenchymal stem cells. *Acta Biomater.* **2021**, *130*, 234–247.

(33) Laurent, S.; Forge, D.; Port, M.; Roch, A.; Robic, C.; Vander Elst, L.; Muller, R. N. Magnetic Iron Oxide Nanoparticles: Synthesis, Stabilization, Vectorization, Physicochemical Characterizations, and Biological Applications. *Chem. Rev.* **2008**, *108*, 2064–2110.

(34) Fortes Brollo, M. E.; Domínguez-Bajo, A.; Tabero, A.; Domínguez-Arca, V.; Gisbert, V.; Prieto, G.; Johansson, C.; Garcia, R.; Villanueva, A.; Serrano, M. C.; Morales, M. d. P. Combined Magnetoliposome Formation and Drug Loading in One Step for Efficient Alternating Current-Magnetic Field Remote-Controlled Drug Release. *ACS Appl. Mater. Interfaces* **2020**, *12*, 4295–4307.